A Comparative Study of Synthesis Processes for LiNi$_{0.5}$Mn$_{1.5}$O$_4$ Cathode Material

Chao Ma[1,], Lei Wang[2], Huanping Yang[3,*], Hong Liu[1]*

[1] College of Electronic Engineering, Chengdu Technological University, Chengdu 611730, China
[2] School of Environmental Science & Engineering, Shanghai Jiao Tong University, Shanghai 200240, China
[3] Zhejiang University of Science & Technology, Hangzhou 310023, China
[*]E-mail: chaoma@yahoo.com, 114026@zust.edu.cn

This work explores the preparation of LiNi$_{0.5}$Mn$_{1.5}$O$_4$, a high voltage cathode material, using the rheological route and two conventional liquid-phase methods. The microstructure of the as-prepared powder materials and the electrochemical performances of LiNi$_{0.5}$Mn$_{1.5}$O$_4$ electrodes are characterized by X-ray diffraction, scanning electron microscopy and electrochemical tests. Although the samples were synthesized through similar methods, the resulting electrochemical properties are quite different. The LiNi$_{0.5}$Mn$_{1.5}$O$_4$ material synthesized via the rheological method not only shows a good cycle performance, but also exhibits the highest discharge capacity of 146.2 mAh g^{-1}. This is mainly ascribed to the combination of solvents in the rheological process which speed up the dispersion and improve the mixability of the precursors, thus inducing the formation of small and uniform electrode particles.

1. INTRODUCTION

Lithium-ion batteries are one of the most successful and promising power sources for meeting the ever-increasing energy demand and relieving from the environmental pollution. Lithium-ion batteries are commercially applied in high power density devices such as electric vehicles or hybrid electric vehicles [1]. Compared with traditional cathode materials such as LiCoO$_2$ (3.9 V), LiMn$_2$O$_4$ (4.1 V) and LiFePO$_4$ (3.5 V), the spinel structure LiNi$_{0.5}$Mn$_{1.5}$O$_4$ allows for a higher voltage (4.7 V) [2]. Among these materials, LiNi$_{0.5}$Mn$_{1.5}$O$_4$ is a promising and attractive one because of its acceptable stability, good cyclic performance and relatively high capacity with a plateau at ~ 4.7 V [3]. The

theoretical capacity of $LiNi_{0.5}Mn_{1.5}O_4$ is 146.7 mAh g^{-1}. Thanks to its high working potential, the energy density of $LiNi_{0.5}Mn_{1.5}O_4$ is 20% higher than that of $LiCoO_2$ [4]; this makes $LiNi_{0.5}Mn_{1.5}O_4$ a promising cathode material for future electric vehicles or energy storage applications [5].

The cathode in lithium-ion battery is well known to rely on insertion/extraction reactions, in which lithium-ions are accommodated into an open host structure allowing for electron accumulation, and the following extraction process corresponds to the electron removal. The cathode material synthesis method plays a significant role in the sample structure and its electrochemical performance. A variety of synthetic methods have been reported for the preparation of cathode materials, including solid state reactions [6], sol-gel [7], co-precipitation [8], rheological [9], spray pyrolysis [10, 11], electrophoretic deposition and pulsed laser deposition [12, 13]. Depending on the preparation procedure, the final product will have a specific microstructure, particle size distribution and phase purity, which will play a vital role in its final electrochemical performance. Therefore, choosing the most appropriate method is essential to prepare high-performance cathode materials.

In this work, the $LiNi_{0.5}Mn_{1.5}O_4$ cathode materials are synthesized via a modified rheological method and via two liquid-phase preparation processes for comparison. The relationship between the preparation route and the electrochemical properties are discussed in details.

2. EXPERIMENTAL

2.1 Materials synthesis

$LiNi_{0.5}Mn_{1.5}O_4$ was prepared by using $Li(CH_3COO) \cdot 2H_2O$ (AR, 99%), $Ni(CH_3COO)_2 \cdot 4H_2O$ (AR, 99%) and $Mn(CH_3COO)_2 \cdot 4H_2O$ (AR, 99%) with the molar ratio of Li: Ni: Mn of 1.05: 0.5: 1.5 (5% excess in molar ratio to compensate for the volatilization of Li during the calcination). The first synthesis route (S1 samples) was the rheological method. The raw materials containing 0.05 mol Li and other metal ions were mixed and grinded thoroughly. Then 10 mL ethanol/distilled water solution was added with the volume ratio of 1: 1, and the mixture was adjusted into a paste. Then, 5 mL of aqueous ammonia (AR, 25%) was added to the mixture and blended to form a brown paste. After being dried at 120 °C, the powders were grinded and compacted, and then calcined at 450 °C for 6 h and at 800 °C for 14 h in air, respectively. Finally, the sample was further annealed at 650 °C for 10 h to fully oxidize the Mn^{3+} into Mn^{4+} [14]. During the whole process, the heating/cooling rate was kept fixed to 5 °C/min.

The second procedure (S2 samples) was based on a liquid-phase method. The same precursor materials were added into 10 mL of distilled water and 5 mL of aqueous ammonia (AR, 25%). Then, a brown paste precursor was formed and let drying and calcinating following the same procedure used for the rheological route.

The third synthesis route (S3 samples) was another liquid-phase method. It used the same raw materials as the rheological method added in only 15 mL anhydrous ethanol solution. A green mushy mixture was obtained after a sufficient mixing time band the rest steps were unvaried respect to the other routes.

2.2 Materials characterization

The crystallization of $LiNi_{0.5}Mn_{1.5}O_4$ powders was investigated by X-ray diffraction (XRD, Bruker D8). The morphology of the $LiNi_{0.5}Mn_{1.5}O_4$ powders was investigated by scanning electron microscopy (SEM, Supra55VP, Zeiss).

2.3 Cell assembly and electrochemical tests

For the electrochemical testing, the cathode was prepared by pasting the slurry containing 80 wt% active materials, 10 wt% conductive carbon black and 10 wt% polyvinylidene fluoride dissolved in 1-methy-1-pyrrolidinone; the mixture was coated onto an Al foil and vacuum dried at 100 °C for 10 h. The electrochemical cells were assembled using the as-prepared cathode, a lithium metal foil counter electrode and porous polypropylene film (Celgard 2400) as separator. The electrolyte solution was 1 M $LiPF_6$ in a solution of ethylene carbonate (EC) and dimethyl carbonate (DMC) (1: 1, v/v). The electrochemical characterization was performed on CR2025 coin-type half-cells in dry Ar-filled glove box.

Charge/discharge tests were performed on a multi-channel battery test system (BTS-51, Neware, China) at room temperature, in the range between 3.5 and 4.9 V and with the current density ranging from 0.2 C to 5.0 C (assuming the theoretical capacity of 150 mAh g^{-1}). The cyclic voltammograms (CVs) were acquired on the CHI650C electrochemical workstation in the potential range from 3.5 to 4.9 V at the scan rate of 0.1 mV s^{-1}.

3. RESULTS AND DISCUSSION

3.1 Material characterizations
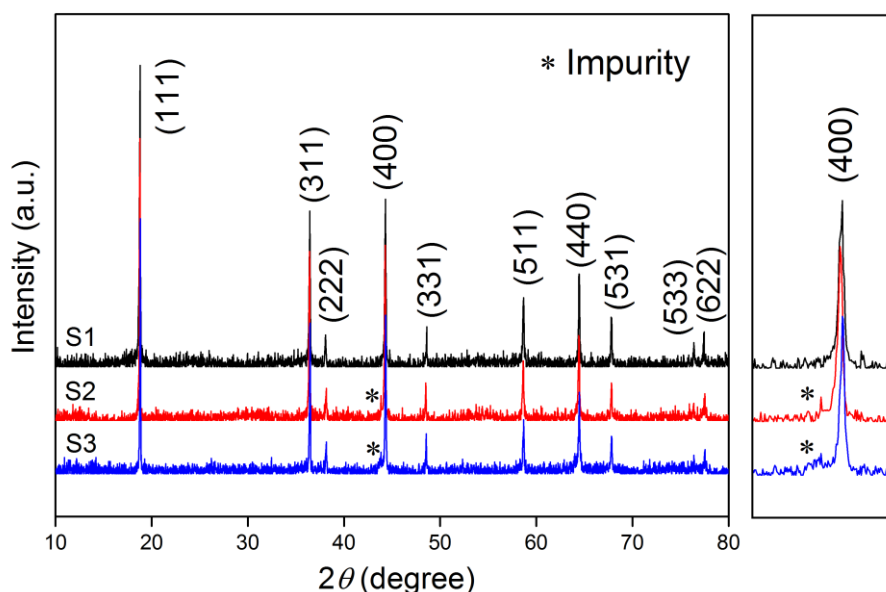
Figure 1. XRD patterns of $LiNi_{0.5}Mn_{1.5}O_4$ powdered samples prepared through the different methods. Impurity peaks are zoomed in the right panel.
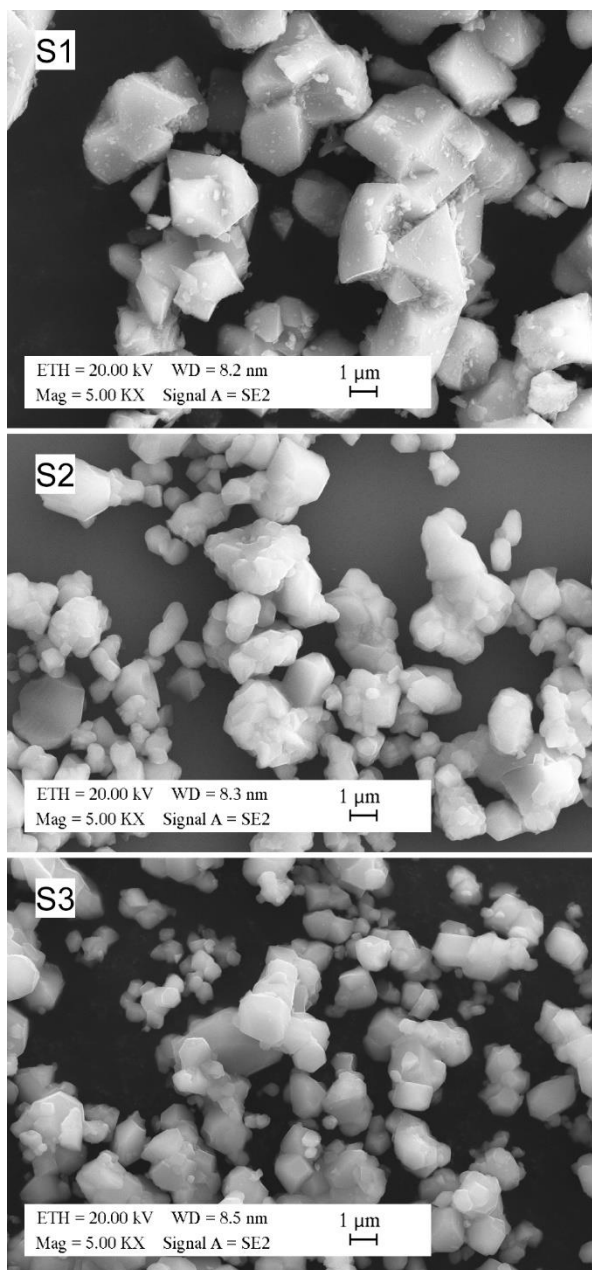
Figure 2. SEM images of $LiNi_{0.5}Mn_{1.5}O_4$ powders obtained by the different preparation methods. The same magnification is applied in each image to compare the particle sizes.

Fig. 1 shows the XRD patterns from $LiNi_{0.5}Mn_{1.5}O_4$ materials fabricated using the three different methods. The main diffraction peaks are labeled according with the *hkl* indices. All diffraction peaks could be assigned to the spinel structure with the space group of *Fd3m*; moreover, the diffraction data well agree with the reference spinel structure of the $LiNi_{0.5}Mn_{1.5}O_4$ compound (according to JCPDS-ICDD 80-2162). The presence of intense and narrow diffraction peaks indicate that well-crystallized spinel structures have been successfully obtained by each method. Sample S1 shows a well-defined cubic spinel structure without any impurity over the full scan range, while S2 and S3 samples obtained through the liquid-phase method display a low amount of impurity-related peaks at $2\theta = 43.8°$, which are ascribed to nickel oxide. Lee and co-workers previously reported that

$LiNi_xMn_{2-x}O_4$ obtained by the liquid-phase method contained NiO impurity [15]. The authors proved that even if a stoichiometric amount of nickel was used in the liquid-phase synthetic process, an extra amount of non-bonded nickel was found in the $LiNi_{0.5}Mn_{1.5}O_4$ powder which could not form the $LiNi_{0.5}Mn_{1.5}O_4$ perfect solid solution and possibly lead to the formation of NiO or $Li_xNi_{1-x}O$ species as seen in the XRD patterns [16].

Fig. 2 shows the SEM images from $LiNi_{0.5}Mn_{1.5}O_4$ samples: samples S2 and S3 show wide particle size distributions between 1 and 3 μm with irregular morphologies, while sample S1 exhibits a regular and homogeneous morphology with an average particle size of about 2 μm. This feature is ascribed to ammonia acting as a chelating agent and allowing the reactants to be mixed uniformly at the molecular level. In addition, the Mn^{2+} would possibly be oxidized to its higher valence state, which would allow to modify the precursor color. Ethanol was used as capping agent thanks to its large dipolar momentum [17], which can reduce the particle agglomeration when used as the solvent. Thus a sufficient dispersion was achieved during the mixture and the following drying procedures. In addition, acetates can dissolve in the distilled water easily and mixed much more sufficiently. The different dispersion and mixability of the precursors may have significant influences on the characteristics of the final products after the heat treatment. However, both S2 and S3 samples lack the required procedures.

3.2 Electrochemical performance
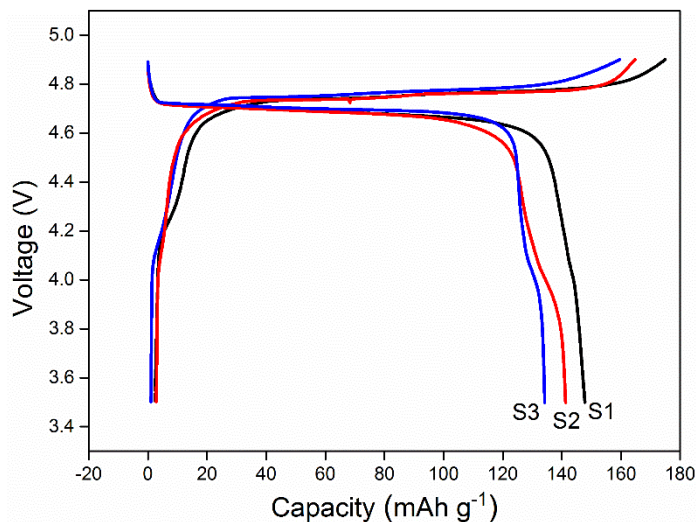
Figure 3. First charge-discharge curves at 0.2 C rate of $LiNi_{0.5}Mn_{1.5}O_4$ electrodes. Two clear voltage plateaus around 4.7 V and 4.1 V can be seen in S1, S2 and S3.

Fig. 3 shows the first charge-discharge curves of $LiNi_{0.5}Mn_{1.5}O_4$ electrodes obtained at 0.2 C rate. For each sample, a voltage plateau is observed at ~ 4.7 V, ascribed to the Ni^{2+}/Ni^{4+} redox reaction. The second plateau at 4.1 V is ascribed to the presence of Mn^{3+} and reflects the Mn^{3+}/Mn^{4+} redox reaction [18]. The highest specific discharge capacity at 0.2 C of 146.2 mAh g^{-1} is obtained for the sample prepared by the rheological method; this value is close to the theoretical capacity. It is remarkable that the discharge voltage plateau around 4.7 V is higher respect to most of similar cathode

materials. Such high discharge voltage not only enhances the energy density but also makes the material capable to be coupled with different anode materials which display better safety-related properties but require high voltage [19]. In addition, $LiNi_{0.5}Mn_{1.5}O_4$ has a relatively high capacity which is similar to the mature commercial olivine $LiFePO_4$ materials, for which the specific discharge at 0.2 C rate is about 162-164 mAh g^{-1}, corresponding to 95.3-96.5% of the theoretical capacity (170 mAh g^{-1}) [20]. However, for $LiFePO_4$ cathodes the voltage plateau occurs at smaller values (~ 3.4 V).
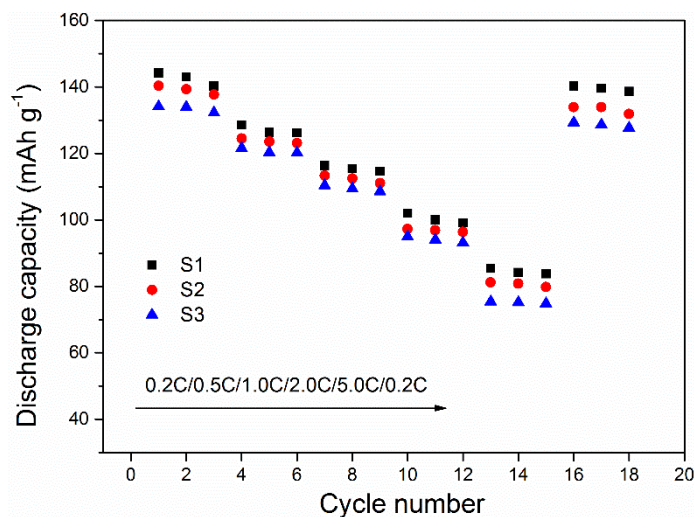

Figure 4. Discharge capacities of $LiNi_{0.5}Mn_{1.5}O_4$ electrodes obtained by the three preparation methods at different discharge rates.

Fig. 4 reports the discharge capacity of $LiNi_{0.5}Mn_{1.5}O_4$ electrodes at different rates. The procedure consists of applying 0.2, 0.5, 1.0, 2.0 and 5.0 C for three charge/discharge cycles followed by the final measurement at 0.2 C (both charge and discharge are performed at the indicated rates). It is not only possible to see the intercalation behavior of the cathode during different discharge rates, but also can understand whether the battery recovers its capacity after the long stress period [21]. Although the three materials are synthesized through similar methods, the electrochemical properties are sensibly different. At 5.0 C, the polarization induced deterioration is observed in the $LiNi_{0.5}Mn_{1.5}O_4$ electrode [22]. The sample S1 displays the best electrochemical stability and reversibility. For S1 sample, the initial discharge capacity at 0.2, 0.5, 1.0, 2.0, 5.0 and 0.2 C rate is 144.2, 128.6, 116.4, 101.9, 85.3 and 140.3 mAh g^{-1}, respectively. After 3 cycles, its discharge capacity at 0.2 C almost recovers to the initial value. For the other two samples (S2 and S3), and the $LiMn_{0.8}Fe_{0.2}PO_4/C$ composite the reversible capacity at 0.1, 0.2, 0.5, 1.0, 2.0, 5.0 and 0.1 C is 142, 123, 114, 103, 91, 69 and 126 mAh g^{-1}, respectively [23]. The optimization of the processing method and conditions of $LiNi_{0.5}Mn_{1.5}O_4$ composite is important for improving the discharge performance; moreover $LiNi_{0.5}Mn_{1.5}O_4$ prepared by rheological method is more tolerant to charge/discharge current rates variation.
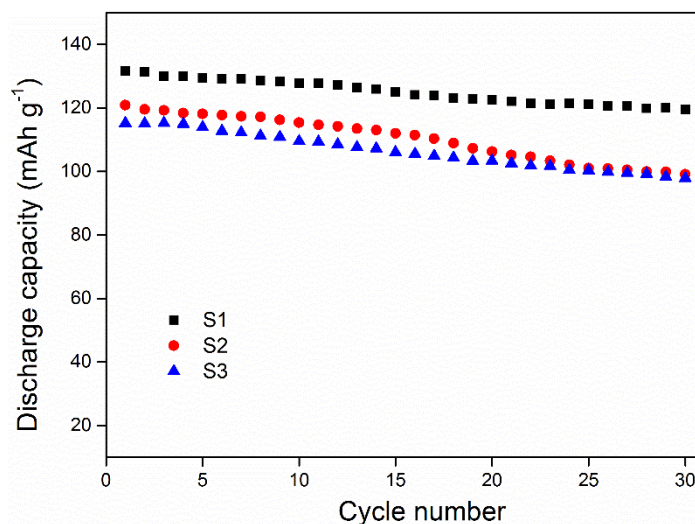
Figure 5. Discharge capacities of $LiNi_{0.5}Mn_{1.5}O_4$ electrodes exposed to continuous cycling at 0.5 C.

Fig. 5 shows the evolution of the discharge capacity of $LiNi_{0.5}Mn_{1.5}O_4$ electrodes upon continuous cycling (30 cycles at 0.5 C rate); S1 exhibits the highest discharge capacity and the best capacity retention during the cycling, with 91% of initial discharge capacity retained after 30 cycles and a capacity loss below 0.4 mAh g^{-1} per cycle. The discharge capacity loss is much higher in S3 (15%) and S2 (18%). For comparison, in a previous research, after 30 cycles at 0.1 C rate, the $LiNi_{1/3}Co_{1/3}Mn_{1/3}O_2$ nanofibers could only retain 88% of their initial discharge capacity [24]. Compared with cathode materials with layered structure, $LiNi_{0.5}Mn_{1.5}O_4$ displays an excellent capacity retention ascribed to the Ni doped spinel $LiMn_2O_4$ structure in which the dissolution of Mn^{2+} into the electrolyte can be avoided [19].
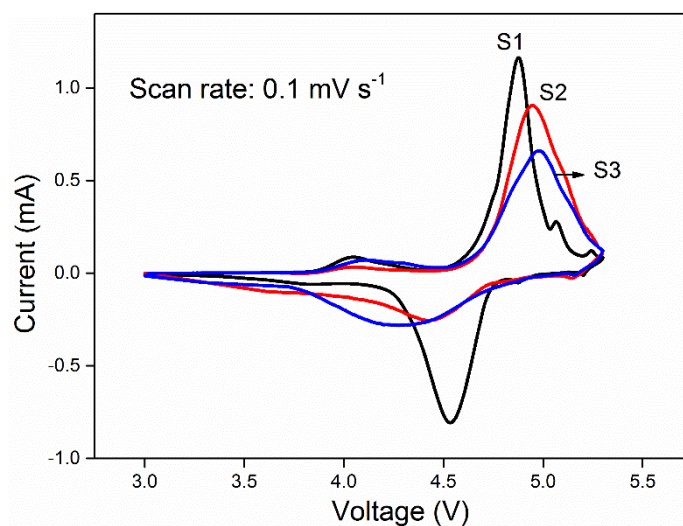
Figure 6. Cyclic voltammograms of $LiNi_{0.5}Mn_{1.5}O_4$ electrodes cycled between 3.0 and 5.3 V vs. Li/Li$^+$ reference electrode at the scan rate of 0.1 mV s^{-1}.

Fig. 6 shows the CVs from $LiNi_{0.5}Mn_{1.5}O_4$ electrodes between 3.0 and 5.3 V. For S1, S2 and S3 samples, the oxidation/reduction peaks occur at 4.53/4.87, 4.42/4.95 and 4.27/4.98 V vs. Li/Li^+, corresponding to the voltage difference of 0.34, 0.53 and 0.71 V, respectively. The redox peaks in S1 show a relatively symmetric profile, indicating a good reversibility of the electrochemical reaction. The potential difference between the redox peaks is quite small and the area surrounded by the CVs is larger for S1 sample, indicating that the electrochemical polarization is relative weak [25]. These characteristics indicate that $LiNi_{0.5}Mn_{1.5}O_4$ electrode synthesized by rheological method has the best electrochemical reversibility and battery reaction kinetics. The small and uniform particle size of $LiNi_{0.5}Mn_{1.5}O_4$ allows for a large surface area which enables Li^+ ions to enter the spinel crystal structure of $LiNi_{0.5}Mn_{1.5}O_4$ electrode with a lower polarization [26]. The improved specific capacity and rate performance is also explained by the increase of efficiency of the electrochemical intercalation and de-intercalation of the Li^+ ions in and out of the host materials thanks to the shorter path length [27].

4. CONCLUSIONS

In summary, $LiNi_{0.5}Mn_{1.5}O_4$ cathode materials are successfully synthesized by rheological and liquid-phase methods and the effects of the synthesis conditions on the final structure, morphology and electrochemical performance have been compared. The modified rheological method uses a chelation reagent to enable the mixing at the molecular level using different reactants. This method leads to the most homogeneous particle size and better electrochemical properties. Small and uniform $LiNi_{0.5}Mn_{1.5}O_4$ electrode particles show a lower agglomeration which can significantly improve the electrochemical stability and the ability to insert and extract much more lithium-ions and electrons efficiently during the cycling. Thus, the $LiNi_{0.5}Mn_{1.5}O_4$ electrode synthesized via the rheological method shows best performance among the three methods in terms of rate capability, reversibility and capacity, in particular at high C-rate. These results demonstrate that $LiNi_{0.5}Mn_{1.5}O_4$ cathode material with high performance can be realized by the improvement of production process.

References

1.   M. Armand, J. M. Tarascon, *Nature*, 451 (2008) 652.
2.   X. Liang, *Int. J. Electrochem. Sci.*, 11 (2016) 4611.
3.   Q. Zhong, A. Bonakdarpour, M. Zhang, Y. Gao, J. Dahn, *J. Electrochem. Soc.*, 144 (1997) 205.
4.   X. Fang, Y. Lu, N. Ding, X. Feng, C. Liu, C. Chen, *Electrochim. Acta*, 55 (2010) 832.
5.   D. Crain, J. Zheng, C. Sulyma, C. Goia, D. Goia, D. Roy, *J. Solid State Electr.*, 16 (2012) 2605.
6.   H. S. Fang, Z. X. Wang, X. H. Li, H. J. Guo, W. J. Peng, *J. Power Sources*, 153 (2006) 174.
7.   H. Liu, Y. Wu, E. Rahm, R. Holze, H. Wu, *J. Solid State Electr.*, 8 (2004) 450.
8.   Y. J. Gu, Q. F. Zang, H. Q. Liu, J. X. Ding, Y. M. Wang, H. F. Wang, J. Zhang, W. G. Wei, *Int. J.*

Electrochem. Sci., 9 (2014) 7712.

9. Q. Liu, H. Liu, X. Zhou, C. Cong, K. Zhang, *Solid State Ionics*, 176 (2005) 1549.
10. S. H. Park, Y. K. Sun, *Electrochim. Acta*, 50 (2004) 439.
11. D. Li, A. Ito, K. Kobayakawa, H. Noguchi, Y. Sato, *Electrochim. Acta*, 52 (2007) 1919.
12. A. Caballero, L. Hernan, M. Melero, J. Morales, R. Moreno, B. Ferrari, *J. Power Sources*, 158 (2006) 583.
13. H. Xia, S. Tang, L. Lu, Y. Meng, G. Ceder, *Electrochim. Acta*, 52 (2007) 2822.
14. R. Santhanam, B. Rambabu, *J. Power Sources*, 195 (2010) 5442.
15. Y. S. Lee, Y. Todorov, T. Konishi, M. Yoshio, *Electrochem. Commun.*, 4 (2002) 989.
16. S. Mukerjee, X. Yang, X. Sun, S. Lee, J. McBreen, Y. Ein-Eli, *Electrochim. Acta*, 49 (2004) 3373.
17. J. E. Martin, J. P. Wilcoxon, J. Odinek, P. Provencio, *J. Phys. Chem. B*, 104 (2000) 9475.
18. D. Guyomard, J. Tarascon, *Solid State Ionics*, 69 (1994) 222.
19. B. Xu, D. Qian, Z. Wang, Y. S. Meng, *Mater. Sci. Eng. R*, 73 (2012) 51.
20. L. Chen, Z. Chen, S. Liu, H. Zhang, Q. Huang, *Int. J. Electrochem. Sci.*, 13 (2018) 5413.
21. J. Xiao, X. Chen, P.V. Sushko, M.L. Sushko, L. Kovarik, J. Feng, Z. Deng, J. Zheng, G.L. Graff, Z. Nie, *Adv. Mater.*, 24 (2012) 2109.
22. T. Ohzuku, R. Yamato, T. Kawai, K. Ariyoshi, *J. Solid State Electr.*, 12 (2008) 979.
23. B. Z. Li, Y. Wang, L. Xue, X. P. Li, W. S. Li, *J. Power Sources*, 232 (2013) 12.
24. Y. Ding, P. Zhang, Z. Long, Y. Jiang, F. Xu, *J. Alloy. Compd.*, 487 (2009) 507.
25. Z. Lu, K. Xueya, T. Wumair, D. Junqing, H. Ying, *J. Power Sources*, 243 (2013) 147.
26. Y. Abu-Lebdeh, I. Davidson, Nanotechnology for Lithium-Ion Batteries, Springer US, (2013) New York, United States.
27. N. Kamarulzaman, R. Yusoff, N. Kamarudin, N. H. Shaari, N. A. Abdul Aziz, M. A. Bustam, N. Blagojevic, M. Elcombe, M. Blackford, M. Avdeev, A. K. Arof, *J. Power Sources*, 188 (2009) 274.